Mon. Not. R. Astron. Soc. **264,** 832–838 (1993)

Morphological classification of galaxies using simple photometric parameters

M. Doi,[1] M. Fukugita[2] and S. Okamura[1]
[1] *Department of Astronomy, University of Tokyo, Tokyo 113, Japan*
[2] *Yukawa Institute, Kyoto University, Kyoto 606, Japan*

Accepted 1993 April 21. Received 1993 March 10; in original form 1993 January 7

ABSTRACT

A simple method is proposed for the morphological classification of galaxies. The method uses two distance-independent photometric parameters, the concentration index and the mean surface brightness within an isophote of fixed brightness level in a single colour band. This method is insensitive both to the image sizes of galaxies and to their inclinations. With this method we achieve a reasonably high success rate ($\gtrsim 85$ per cent) in classifying galaxies into early and late types. We demonstrate that the method works well for galaxies near the observational limit of automated galaxy surveys.

Key words: methods: data analysis – galaxies: fundamental parameters – galaxies: photometry.

1 INTRODUCTION

Morphological classification of galaxies has traditionally been carried out by visual inspection of images according to Hubble's classification scheme (Sandage 1961). With the advent of automated digitized galaxy surveys, however, it is now highly desirable to find a quantitative criterion with simple photometric parameters for morphological classification. There are a number of parameters, such as colour, bulge-to-disc ratio, gaseous content, etc., that are known to exhibit a good correlation with morphological type. There have been a few attempts to use some of these parameters to characterize morphological types (e.g. de Vaucouleurs 1977a; Okamura, Kodaira & Watanabe 1984, hereafter OKW), but no attempts actively to use them to classify galaxies.

The first method that one might consider is to use the growth curve of aperture photometry (e.g. de Vaucouleurs 1977b; de Vaucouleurs, de Vaucouleurs & Corwin 1976, hereafter RC2) and examine which model curve fits the brightness profile better: early-type galaxies are known to obey de Vaucouleurs' $r^{1/4}$ law (de Vaucouleurs 1948), and late-type galaxies show an exponential decay of surface brightness (Freeman 1970). It turns out, however, that the growth curve for spiral galaxies depends rather strongly on the inclinations of the galaxies, which makes it difficult to distinguish highly inclined spirals from early-type galaxies. In fact, the method that uses the goodness of fit of the growth curve does not work well in practical applications. De Vaucouleurs & Agüero (1973) (see also de Vaucouleurs 1977a) discussed a primitive classification that uses the concentration index. OKW subsequently showed that early- and late-type galaxies are separated well by the use of the mean surface brightness and an index related to the central concentration of luminosity. The concentration index they used is, however, defined by parameters obtained from the principal component analysis of galaxy images, and is too complicated for practical use in galaxy surveys; in particular, the method cannot be applied to distant galaxies with small images. Recent attempts to classify galaxies into morphological types by employing pattern recognition algorithms, using a number of photometric parameters (with the aid of fuzzy algebra) to categorize similar galaxies (Spiekermann 1992), or more recently using artificial neural networks, represent effort in a different direction (Storrie-Lombardi et al. 1992).

In this paper we propose a conceptually simple method that uses photometric parameters for the morphological classification of galaxies, and test its validity for some practical cases. Our idea, like the test by OKW, is to detect the central concentration of luminosity in elliptical galaxies and the disc extension of spiral galaxies by looking at the correlation between the concentration index and the mean surface brightness. Our method involves simple distance-independent photometric parameters only and, it is hoped, applies to small and faint galaxy images of rather poor image quality. We show that our method works to the extent that one can at least separate early- and late-type galaxies with a high probability.

In Section 2 we describe the method. The test is reported in Section 3, first using a nearby galaxy sample, and then using a more distant galaxy sample from the Coma cluster. A

preliminary version of the present work is reported in Doi et al. (1992).

2 THE METHOD

We base our definition of the equivalent radius $r(\mu)$ on the number of pixels $n(\mu)$ that have a flux that exceeds the surface brightness μ:

$$n(\mu)\,\Delta S=\pi r(\mu)^2, \tag{1}$$

with ΔS the pixel area. We then define the concentration index parameter $c_{\rm in}(\alpha)$ by

$$c_{\rm in}(\alpha)=\int_0^{\alpha r(\mu_L)} rI(r)\,{\rm d}r \Big/ \int_0^{r(\mu_L)} rI(r)\,{\rm d}r, \tag{2}$$

where $2\pi rI(r)\,{\rm d}r$ is the differential flux between r and $r+{\rm d}r$, $I(r)$ is the equivalent profile (areal profile), and α is a parameter $0<\alpha<1$ chosen appropriately. We take μ_L to be the detection threshold.

We adopt the conventional definition of mean surface brightness. We denote by SB_μ the mean surface brightness averaged over the isophote of brightness μ, and plot galaxies on the $c_{\rm in}$–SB_{μ_L} plane. Here both $c_{\rm in}$ and SB_{μ_L} are distance-independent parameters.

Let us show that galaxies with a de Vaucouleurs profile and those with an exponential profile occupy completely separate regions on the $c_{\rm in}-SB_{\mu_L}$ plane. In Fig. 1 we draw two curves (thick solid curves), which correspond respectively to de Vaucouleurs' law

$$I(r)=I_{\rm e}\exp[-7.67(r/r_{\rm e})^{1/4}-1] \tag{3}$$

and the exponential law

$$I(r)=I_{\rm e}\exp[-(r/r_{\rm e})], \tag{4}$$

for the choice $\alpha=0.3$ and $\mu_L=25.5$ mag arcsec^{-2}. Ticks on the curves show the values of $\mu_{\rm e}=-2.5\log I_{\rm e}$ indicated in the figure.

We note that the position of the curve depends only on the profile of the galaxies. We also see that the curve is rather insensitive to inclination for spiral galaxies. High inclination acts to increase surface brightness, and also, to a lesser extent, to increase $c_{\rm in}$. As a result, the direction of the shift on the (SB_μ, $c_{\rm in}$) plane due to inclination is close to that of the curve expected for exponential discs, and hence this shift is almost in the direction of the distribution of spiral galaxies. We show this in Fig. 1, where we plot a segment (dashed curve) that shows the effect of inclination for a spiral with $\mu_{\rm e}=21.5$ mag arcsec^{-2}, assuming that spiral discs are optically thin. Correction for inclination is therefore not important; this is a crucial point for the successful classification of types, as discussed below.

The position of the curve is slightly affected by seeing. To illustrate this point, we also present in Fig. 1 the way in which the curves are affected by finite seeing, which is assumed to take the Gaussian form of $\exp[-(r_{\rm e}/\sigma)^2/2]$. A few curves (thin curves) are drawn for different choices of $\gamma=\sigma/r_{\rm e}$. The seeing effect generally shifts the curve downwards, and would reduce the power of discrimination for low surface brightness galaxies. For the examples that we shall consider here, however, this effect is not too serious.

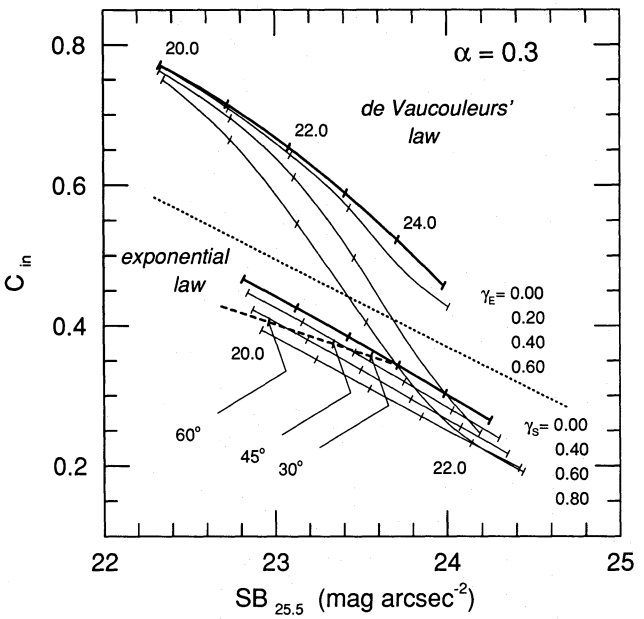

Figure 1. Positions on the ($c_{\rm in}$, $SB_{25.5}$) plane expected for galaxies with de Vaucouleurs' profile (equation 3; upper thick curve) and for those with the exponential profile (equation 4; lower thick curve) for the case of $\alpha=0.3$. Ticks on the curves show $\mu_{\rm e}$. Thin curves are the positions expected with corrections for finite seeing ($\gamma=\sigma/r_{\rm e}$). The thick dashed line represents the shift for inclined spirals for the case $\mu_{\rm e}=20.5$ mag arcsec^{-2}. The dotted line is a separation line used for classification, as explained in the text.

3 APPLICATION OF THE METHOD

3.1 Nearby galaxy sample

Let us first demonstrate the effectiveness of the method by applying it to a nearby galaxy sample. We take the sample from the Photometric Atlas of Northern Bright Galaxies (Kodaira, Okamura & Ichikawa 1990, hereafter PANBG), which provides good photographic surface photometry in the V band for 791 galaxies taken from the Revised Shapley–Ames Catalog of Bright Galaxies (Sandage & Tammann 1981, hereafter RSA). More than 95 per cent of the 791 galaxies have $V_T<13.5$ mag.

In Fig. 2 the distribution of the 789 PANBG galaxies is plotted on the $c_{\rm in}$–SB_{μ_L} plane with $\alpha=0.3$. The surface brightness threshold is set equal to $\mu_L(V)=24.5$ mag arcsec^{-2}. Different morphological types are plotted with the symbols specified in Table 1. Similar plots are given in Fig. 3 for each morphological type separately to avoid clutter. The correction for finite seeing is unimportant in this case.

We observe from Fig. 2 (and from Fig. 3) that the galaxy plots are largely divided into two components, the upper component corresponding to early-type galaxies and the lower one to late-type galaxies. Looking more closely at the figure one can see that ellipticals are distributed in a narrow region close to the curve represented by equation (3). Galaxies of E/S0–S0/a types are more scattered, but are mostly in the upper component. The types Sa–Sa/b are located in the middle, extending from the upper to the lower components. The late types Sb–Im also show a scattered distribution, but are almost confined to the lower component.

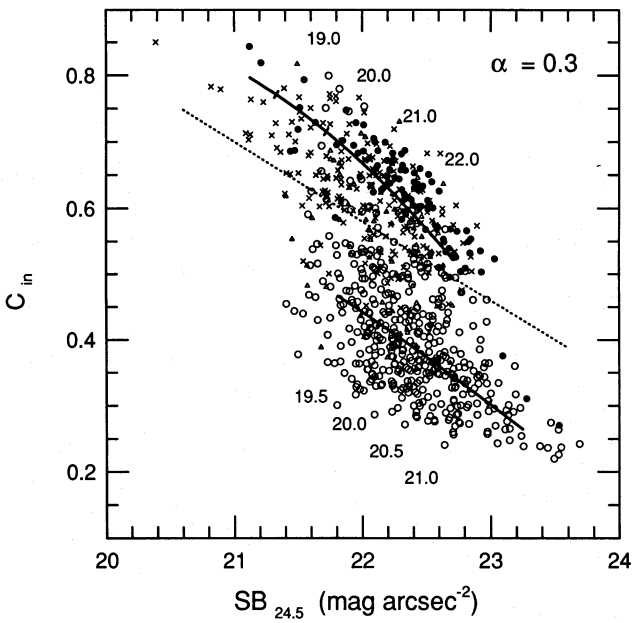

Figure 2. Plot of 789 PANBG galaxies on the (c_{in}, $SB_{24.5}$) plane. The symbols used are explained in Table 1. The two solid curves show the positions expected for galaxies with de Vaucouleurs' profile and for those with the exponential profile for zero seeing. The dotted line is the line given by equation (5) that was used for our provisional classification.

Table 1. Adopted classification scheme for morphological types.

Hubble type	T(RSA)	symbol
E	−6 – −4	solid circle
E/S0 – S0/a	−3 – 0	cross
Sa – Sa/b	1 – 2	open triangle
Sb – Im	3 – 10	open circle

It is easy to see that ellipticals and spirals later than Sb are separated almost completely at a level of 95 per cent. E/S0–S0/a are also separated from late spirals, with contamination at the 10 per cent level. On the other hand, it is not easy to separate Sa–Sa/b either from earlier or from later types. It is also difficult to separate E/S0–S0/a from ellipticals.

Here we attempt to classify galaxies into only two types, early types (E–S0/a) and late types (Sb–Im), allowing for some contamination from Sa galaxies. This is a rudimentary classification, but even so is still useful, because S0s share many of the characteristics of ellipticals, and it is often sufficient to classify galaxies into early and late types. We provisionally define the galaxies located above the line

$$c_{in} = -0.12SB + 3.22 \qquad (5)$$

as 'early'-type, and those below as 'late'-type. We then compare them to the types given in the RSA. Table 2 shows the numbers of E, E/S0–S0/a, Sa–Sa/b and Sb–Im galaxies that are classified into 'early' and 'late' types according to our definition. The numbers in parentheses show success (with underlines) and failure percentages for each type. As expected, 94 per cent of ellipticals are correctly classified as early-type. Of the remaining 6 per cent, half are dwarf spheroidals with low surface brightness, for which the adequacy of the classification is suspect; intrinsic differences are known to exist between the surface brightness distribution of normal ellipticals and that of dwarf spheroidals that are usually classified as ellipticals (Binggeli, Sandage & Tarenghi 1984; Ichikawa, Wakamatsu & Okamura 1986). E/S0–S0/a and Sb–Im are classified as early- and late-type, respectively, at the 90 per cent level. 50 per cent of Sa–Sa/b are classified as early-type, and the other 50 per cent as late-type. The overall success rate of separation is about 85 per cent for both the early (earlier than S0/a) and late (later than Sa) types.

We also tried a similar analysis using $\alpha = 0.1$, with the expectation that the two types would be separated more clearly. Fig. 4 shows, however, that this is not the case; the distribution of ellipticals is more widely scattered, whereas that of spirals is slightly narrower. The former distribution is a result of the fact that the light concentration at the very centre of ellipticals varies wildly from galaxy to galaxy, and the concentration parameter shows a much better correlation with surface brightness when integrated over an extended region. For spiral galaxies, a smaller α samples the light in the region at the very centre of the bulge, and the resulting c_{in} does not provide much information on the bulge-to-disc ratio. As a result, the separation is hardly improved, and may even be made worse, by choosing a smaller α. A smaller α is observationally more demanding for distant galaxies, and also renders the separation more susceptible to seeing variations. If, on the other hand, α is chosen to be larger than 0.3, the separation gradually worsens. We therefore conclude that $\alpha = 0.3$ is the optimal choice from the viewpoint of practical applications.

3.2 Coma cluster galaxies

In order to see whether this method works for galaxies with small image sizes, we tested it with photometric data from plates of the Coma cluster region taken with the Kiso Schmidt telescope (see Fukugita et al. 1991 for details). Kodak IIa-O plates were used behind a Schott GG-385 filter. The image scale was 62.5 arcsec mm^{-1}. We carried out automated image reduction for five plates covering a region of $9\overset{\circ}{.}8 \times 9\overset{\circ}{.}8$ centred on NGC 4874 using AIMS software as described in Doi, Fukugita & Okamura (1993). The detection threshold was set at $\mu_L(B) = 25.5$ mag arcsec^{-2}. The seeing size varied between 3.6 and 4.3 arcsec, and was increased effectively by 25 per cent with a smoothing procedure. The limiting magnitude for the detection of stars is about 19.5 mag, and star–galaxy discrimination can be achieved down to 17.5 mag with a contamination of about 3 per cent. We restrict our analysis here to galaxies brighter than 16 mag for two reasons: the first is that few galaxies fainter than 16 mag are given morphological types in existing catalogues. The second reason is that the effect of seeing becomes significant beyond 16 mag in our surface photometry. With this criterion we detected 501 galaxies, half of which have magnitudes between 15 and 16 mag. We refer the reader to Doi, Fukugita & Okamura (1993) for more details. Due to poor seeing, 16 mag was a practical limit for galaxy surface photometry, and the test described below was performed for galaxies close to this limit. In our analysis we excluded galaxies with blended images, which leaves 338 galaxies in our sample.

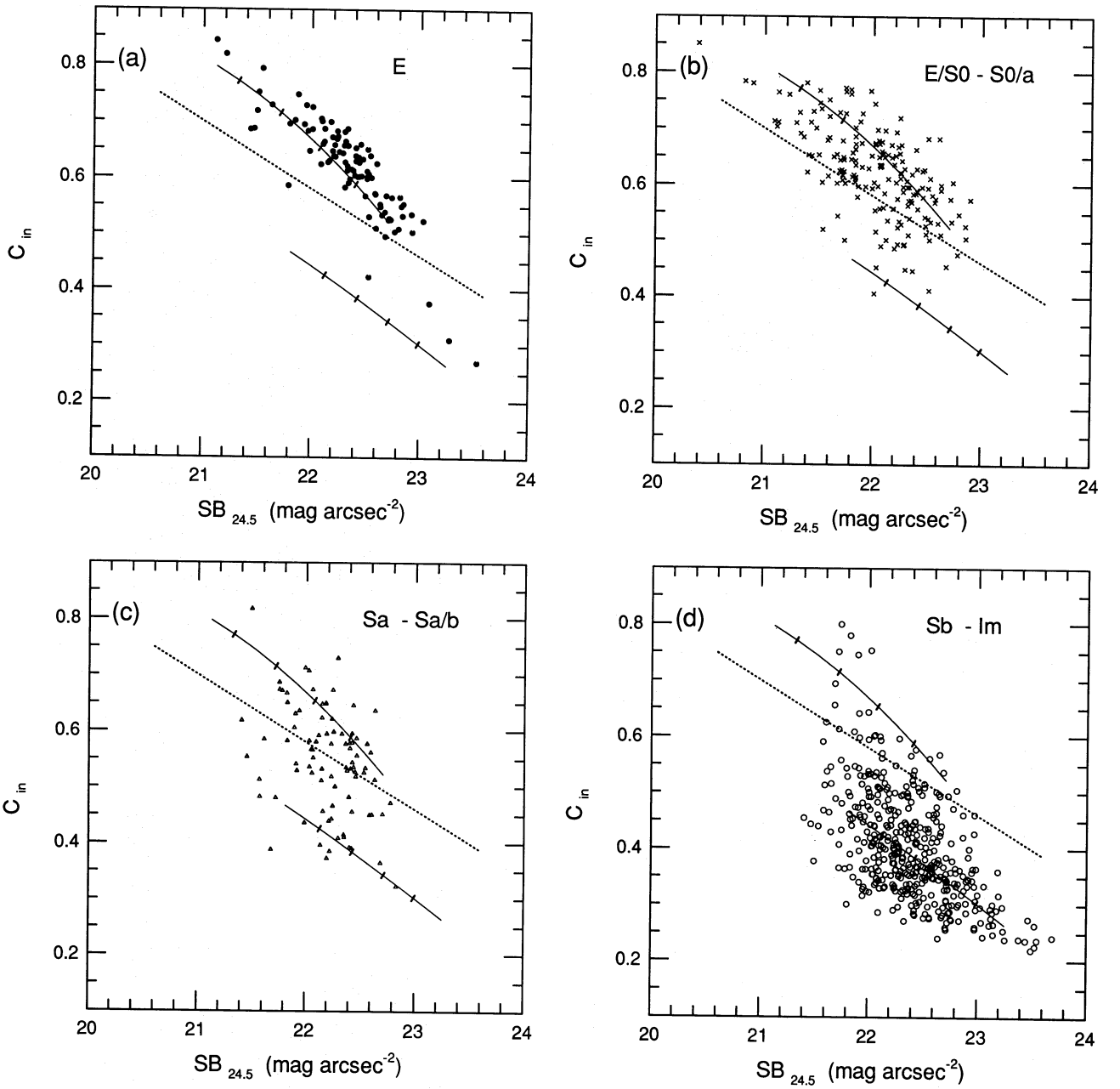

Figure 3. As Fig. 2, but E, E/S0–S0/a, Sa–Sa/b and Sb–Im galaxies are plotted separately in (a), (b), (c) and (d) respectively.

Table 2. Classification of morphological types for 789 nearby galaxies.

		"early"		"late"	
E	98	92 (94%)	} 241 (85.5%)	6 (6%)	}41 (14.5%)
E/S0 – S0/a	184	149 (81%)		35 (19%)	
Sa – Sa/b	87	44 (51%)	}69 (14%)	43 (49%)	} 435 (86%)
Sb – Sm	420	28 (7%)		392 (93%)	

The first test was carried out with 114 galaxies that were given morphological types by de Vaucouleurs et al. (1991, hereafter RC3), and that are positionally identified with those in RC3 within an error of 15 arcsec. The galaxies are plotted in Fig. 5 using the same symbols as in Fig. 1 except that early spirals are not distinguished from late spirals and are classified merely as spirals. The basic characteristics seen in this figure are the same as those in Fig. 2 for nearby galaxies, in spite of the differences in the image size and in the colour band. A small downward shift of the galaxy distributions compared with the two expected curves may be understood as a result of finite seeing. Indeed, we expect $\gamma_E \approx 0.3$ for early types and $\gamma_S \approx 0.6$ for late types for typical galaxies in the Coma cluster, and these corrections bring the curves in Fig. 5 to the middle of the observed distributions (see Fig. 1). We then try to separate galaxies into early and late types by drawing a line,

$$c_{in} = -0.125SB + c_0, \qquad (6)$$

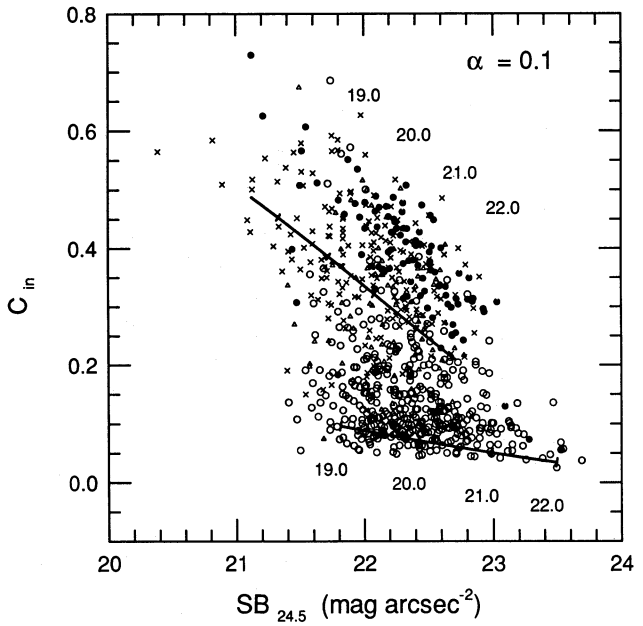

Figure 4. As Fig. 2 for $\alpha = 0.1$.

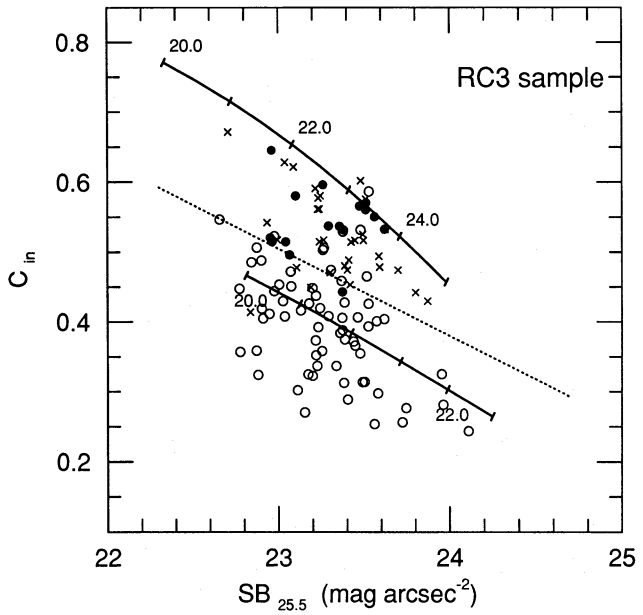

Figure 5. Plot of 114 Coma galaxies listed in RC3 on the (c_{in}, $SB_{25.5}$) plane. The symbols used are explained in Table 1, except that early-type spirals are not distinguished from late-type spirals, spirals being denoted by open circles. The two thick curves are curves given by equations (3) and (4), and represent the positions expected for the zero-seeing case. The dotted line represents the line given by equation (6) that was used for our classification.

with the optimal choice $c_0 = 3.38$. The score for our classification is presented in Table 3. We see that 88 per cent of ellipticals and 88 per cent of spirals are correctly classified. 91 per cent of S0s are also classified as early type. On the other hand, 16 per cent of galaxies classified as early type are spiral galaxy contaminants, and 8 per cent of galaxies classified as late type are misidentified ellipticals or S0s. If c_0 is

Table 3. Classification of morphological types for RC3 galaxies in the Coma region.

RC3 type		"early"		"late"	
E	16	14 (88%)	43 (90%)	2 (12%)	5 (10%)
S0	32	29 (91%)		3 (9%)	
S+I	66	8 (12%)		58 (88%)	

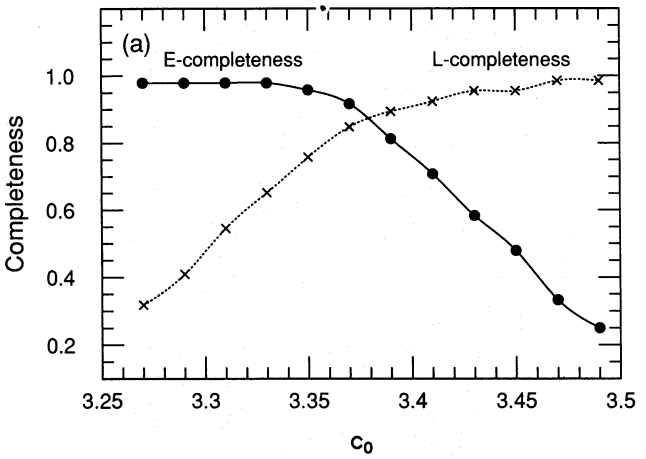

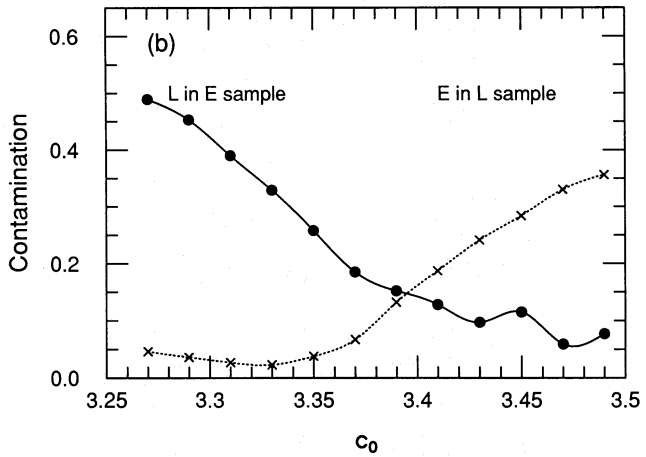

Figure 6. (a) Completeness of the early (E) and late (L) galaxy samples as obtained by the method proposed in the text, as a function of c_0. (b) Contamination by the other class of the early- and late-type galaxy samples as a function of c_0.

taken to be 3.42, the contamination by spirals of the early-type galaxy sample reduces to about 10 per cent, although there is a loss of 35 per cent of the early-type galaxies. For the late-type galaxy sample, completeness of more than 80 per cent is achieved, allowing for a 10 per cent contamination from early-type galaxies. Fig. 6 shows the fractional contamination and completeness of the early- and late-type samples as a function of c_0. Appropriate values of c_0 can be chosen in accordance with the investigator's purpose.

A similar analysis was carried out using 42 galaxies catalogued in Nilson (1973, hereafter UGC), and the results are presented in Table 4. The same line was used for separation of types. The features of the results are very similar to those

Table 4. Classification of morphological types for UGC galaxies in the Coma region.

UGC type		"early"		"late"	
E	2	2 (100%)	} 17 (100%)	0 (0%)	}0 (0%)
S0	18	18 (100%)		0 (0%)	
S+I	22	1 (4%)		21 (96%)	

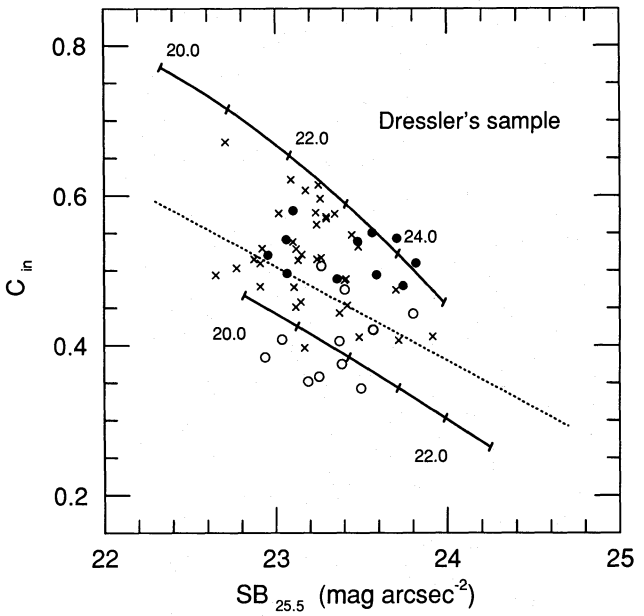

Figure 7. Plot of 60 Coma galaxies identified with those listed in Dressler's sample. The details are as for Fig. 5.

Table 5. Classification of morphological types for the Dressler sample in the Coma region.

Dressler type		"early"		"late"	
E	11	10 (91%)	} 35 (73%)	1 (9%)	}13 (27%)
S0	37	25 (69%)		12 (32%)	
S+I	12	3 (25%)		9 (75%)	

for RC3, and the success rate of morphological separation is even higher.

We have also applied a similar test to 60 galaxies which were given morphological types by Dressler (1980) (see Fig. 7). The separation is somewhat worse than in the RC3 and UGC cases, if the same criterion is taken for separation; a significant number of S0s fall below the line (see Table 5). The success rate, however, recovers almost to the same level as for RC3 if we draw the separation line slightly lower ($c_0 = 3.34$).

4 DISCUSSION

We have shown that we are able to separate galaxies into early and late types using simple distance-independent photometric parameters with a reasonable success rate ($\gtrsim 85$ per cent). We have demonstrated that the method works well for galaxies of small image size that are rather close to the limits of observation. It is also possible to keep the contamination in the early-type galaxy sample to less than 10 per cent, if we sacrifice completeness to a level of 60–70 per cent. For the late-type galaxy sample, better completeness (> 80 per cent) is obtained by allowing for a 10 per cent contamination from early-type galaxies. We remark that the present method is rather insensitive to reddening, colour band and image size as well as to the effect of inclination. In particular, the insensitivity to the effect of inclination explains why we could successfully classify galaxies into early and late types, whereas the more direct method based on fitting the growth curve does not work well. An advantage of the present method over other attempts that exploit pattern recognition algorithms (Spiekermann 1992; Storrie-Lombardi et al. 1992) is that only two conceptually simple parameters are used. We remark that the present method may also apply to the machine-based output of galaxy images that are routinely produced, for example, by APM and COSMOS, if an adequate interpolation is made among equivalent profiles at different isophotal levels. One might suppose that the present method may be used for star–galaxy discrimination. We have checked this possibility, but found that this method is not particularly superior to existing star–galaxy discrimination algorithms (e.g. Heydon-Dumbleton, Collins & MacGillivray 1989).

Similar classifications may be carried out with parameters other than those used in this paper, provided that the parameters are sensitive to the difference between the two laws of galaxy light distributions and are not too sensitive to the effect of inclination. For example, the surface brightness parameter SB_{μ_L} may be replaced with μ_e, the surface brightness at the effective radius r_e. The success rate of classification hardly changes with this choice. The parameter c_{out}, as defined by

$$c_{\rm out}(\alpha_1,\alpha_2)=\frac{1-\alpha_2^2}{\alpha_2^2-\alpha_1^2}\left[\int_{\alpha_1 r(\mu_L)}^{\alpha_2 r(\mu_L)} rI(r)\,{\rm d}r \Big/ \int_{\alpha_2 r(\mu_L)}^{r(\mu_L)} rI(r)\,{\rm d}r\right], \qquad (7)$$

may also be used instead of c_{in}, and galaxies may be plotted on the c_{out}–SB plane. Here c_{out} is the ratio of the average surface brightness between the fractional equivalent radii α_1 and α_2 to that between α_2 and 1. This method has the merit that c_{out} may often be measured more reliably than c_{in}, which may suffer from saturation for high surface brightness galaxies, especially when photographic surface photometry is used. We show in Fig. 8 a plot on the $c_{out}(0.6, 0.8)$–SB_{μ_L} plane corresponding to Fig. 2. We find that separation is achieved at a level almost equal to that using c_{in}–SB for high surface brightness galaxies. For lower surface brightness galaxies, however, we find more confusion than in Fig. 2. We conclude that the plot c_{in}–SB_{μ_L} is the best of those we tested.

We finally compare our results with those of Spiekermann (1992), who carried out the most elaborate attempt to date at the automated classification of morphological types. While his classification algorithms and measured parameters are apparently much more elaborate and detailed, we find that our present method is as effective as his, in so far as early–late separation is concerned. For instance, the percentage of E–S0/a (our early types) classified correctly as early type is 71 per cent for $14 \lesssim m \lesssim 15$ mag, and drops to 29 per cent for $15 \lesssim m \lesssim 16$ mag in his analysis. In our analysis a

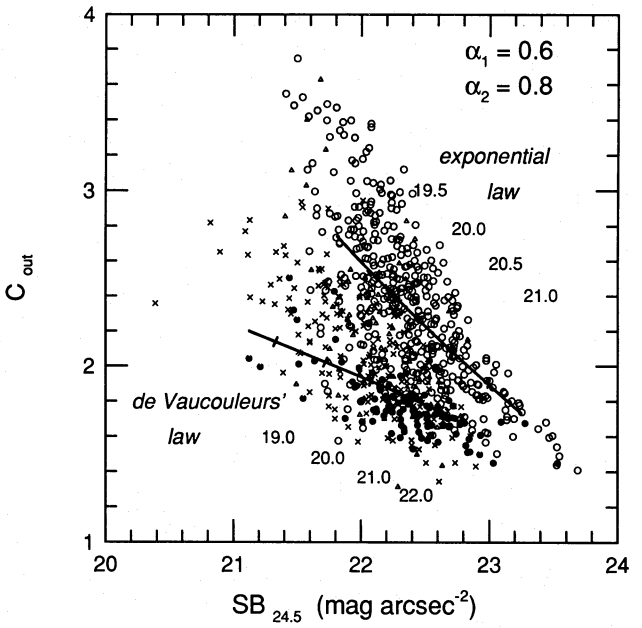

Figure 8. Plot of 789 PANBG galaxies in the (c_{out}, $SB_{24.5}$) plane with $\alpha_1 = 0.6$ and $\alpha_2 = 0.8$. The symbols used are explained in Table 1.

success rate higher than 80 per cent is sustained to 16 mag in spite of much poorer seeing on our plates. The average overall success rate in Spiekermann's analysis is 85 per cent for $14 \lesssim m \lesssim 15$ mag and 91 per cent for $15 \lesssim m \lesssim 16$ mag, but these high values are largely due to the spiral dominance (75–85 per cent) in his sample.

The positions of spirals on the c_{in}–SB_{μ_L} plane show a reasonable correlation with their subtypes. With our method it is indeed possible to subdivide spirals into Sa, Sb, Sc, etc., if one accepts a substantial rate of misclassification (say ~50 per cent) into neighbouring classes. We expect that the success rate of this subclassification will not be much worse than that by Spiekermann. For early types, however, E and S0 are hardly discriminated by our present method.

As a concluding remark, we suggest that it would not be easy to find objective and quantitative criteria that could achieve better classification than that presented here, in so far as we take the conventional morphological types as adopted in the existing catalogues. This is chiefly because the conventional criteria (Sandage 1961) are concerned with astrophysically hybrid aspects of galaxies: the fundamental framework of the galaxy, which is represented by the bulge-to-disc ratio criterion; and the star formation activity, which is represented typically by the openness of the spiral arms and the degree of resolution into stars, H II regions, etc. To proceed further we might have to set some criteria so that morphological types are defined in a quantitative way by use of photometric parameters; such criteria should make it easier to compare theoretical arguments with observations.

ACKNOWLEDGMENTS

We thank Alan Dressler for providing his cluster catalogue in a machine-readable form, and K. Tarusawa for his help in PDS scanning of Schmidt plates. We are also grateful to Edwin Turner for useful comments on improving the manuscript. Part of the computations was carried out at the Astronomical Data Analysis Centre of the National Astronomical Observatory, Tokyo.

REFERENCES

Binggeli B., Sandage A., Tarenghi M., 1984, AJ, 89, 64
de Vaucouleurs G., 1948, Ann. Astrophys., 11, 247
de Vaucouleurs G., 1977a, in Tinsley B. M., Larson R. B., eds, The Evolution of Galaxies and Stellar Populations. Yale University Observatory, New Haven, p. 43
de Vaucouleurs G., 1977b, ApJS, 33, 211
de Vaucouleurs G., Agüero E., 1973, PASP, 85, 150
de Vaucouleurs G., de Vaucouleurs A., Corwin H. G., Jr, 1976, Second Reference Catalogue of Bright Galaxies. University of Texas Press, Austin (RC2)
de Vaucouleurs G., de Vaucouleurs A., Corwin H. G., Jr, Buta R. J., Paturel G., Fouqué P., 1991, Third Reference Catalogue of Bright Galaxies. Springer-Verlag, New York (RC3)
Doi M., Fukugita M., Okamura S., 1993, Kyoto preprint YITP/K-1000
Doi M., Kashikawa N., Okamura S., Tarusawa K., Fukugita M., Sekiguchi M., Iwashita H., 1992, in MacGillivray H. T., Thomson E. B., eds, Digitised Optical Sky Surveys. Kluwer, Dordrecht, p. 199
Dressler A., 1980, ApJS, 42, 565
Freeman K., 1970, ApJ, 160, 811
Fukugita M., Okamura S., Tarusawa K., Rood H. J., Williams B. A., 1991, ApJ, 376, 8
Heydon-Dumbleton N. H., Collins C. A., MacGillivray H. T., 1989, MNRAS, 238, 379
Ichikawa S., Wakamatsu K., Okamura S., 1986, ApJS, 60, 475
Kodaira K., Okamura S., Ichikawa S. (eds), 1990, Photometric Atlas of Northern Bright Galaxies. University of Tokyo Press, Tokyo (PANBG)
Nilson B., 1973, Uppsala General Catalogue of Galaxies, Acta Uppsala Univ., Ser V: A, Vol. 1 (UGC)
Okamura S., Kodaira K., Watanabe M., 1984, ApJ, 280, 7 (OKW)
Sandage A., 1961, The Hubble Atlas of Galaxies. Carnegie Institution of Washington, Washington DC
Sandage A., Tammann G. A., 1981, A Revised Shapley-Ames Catalog of Bright Galaxies. Carnegie Institution of Washington, Washington DC
Spiekermann G., 1992, AJ, 103, 2102
Storrie-Lombardi M. C., Lahav O., Sodré L., Storrie-Lombardi L. J., 1992, MNRAS, 259, 8P